Continental Shelf Research 57 (2013) 10–17

Contents lists available at SciVerse ScienceDirect

Continental Shelf Research

journal homepage: www.elsevier.com/locate/csr

Research papers

# Distribution patterns of particle-reactive radionuclides in sediments off eastern Hainan Island, China: Implications for source and transport pathways

Dekun Huang, Jinzhou Du*, Bing Deng, Jing Zhang

State Key Laboratory of Estuarine and Coastal Research, East China Normal University, Shanghai 200062, China

ARTICLE INFO

*Article history:*
Received 1 April 2011
Received in revised form
20 April 2012
Accepted 26 April 2012
Available online 5 May 2012

*Keywords:*
Sediment transport
Sediment sources
Particle-reactive radionuclides
Hainan Island

ABSTRACT

The study of sediment sources and transport processes from land to ocean can help in predicting the fate of the pollutants released from land or the potential change in sediment delivery to coastal areas and/or open oceans. The activities of $^{7}$Be, excess $^{210}$Pb ($^{210}Pb_{xs}$), excess $^{234}$Th ($^{234}Th_{xs}$) and $^{137}$Cs in surface sediments collected offshore of eastern Hainan Island, China, in August of 2008 were measured by an HPGe $\gamma$-spectrometer to evaluate the sediment source and transport processes. The results showed that all the surface sediments were silt or sand, and the mean grain sizes of the northern locations were higher than those in the other regions. The ranges of activities of $^{7}$Be, $^{210}Pb_{xs}$, $^{234}Th_{xs}$ and $^{137}$Cs in surface sediment were 0.14–12.7, 37.4–199, 2.24–176 and 0.02–1.06 Bq kg$^{-1}$, with averages of $3.78 \pm 4.77$, $110 \pm 8.1$, $66.7 \pm 8.9$ and $0.52 \pm 0.22$ Bq kg$^{-1}$, respectively. The activities of the radionuclides increased from coast to offshore in the northern section. The upwelling may cause high particle fluxes with high activities of $^{210}Pb_{xs}$ and $^{234}Th_{xs}$. A comparison of the source and transport of the suspended sediments with river discharge along the coast shows that the coastal current and offshore upwelling are the dominant factors for the transport and sources of surface sediment in the study region. The sediment was transported from south to north by the coastal current, and sediments with a large grain size may be deposited via the north loop current. The ratios of the nuclide activities indicated that the suspended particles need approximately one year to be removed from the water column into the seabed and that the main source of the sediments off eastern Hainan Island in the study regions was terrigenous deposits.



## 1. Introduction

Understanding the sediment sources and transport processes from land to ocean can help with predicting the fate of land pollutant release or potential change in sediment delivery to coastal areas and/or open oceans. Moreover, pollutant-bearing fine sediment can move slowly through a river/estuary system in a series of steps associated with cycles of deposition and resuspension during the different hydrological stages (Sanford, 1992). These pollutants may also have a significant impact in receiving areas, such as estuaries and oceans, and the linkage between river drainage basins and the ocean is important for water quality (Saari et al., 2010).

Natural and artificial radionuclides can be utilized with success to investigate the movement of suspended sediments and dissolved materials in estuarine, coastal and marine environments (Santschi et al., 1999; Baskaran and Santschi, 2002; Yeager et al., 2004; Hong et al., 2006; Burnett et al., 2008; Moore and de Oliveira, 2008; Xu et al., 2010; Su et al., 2011). To examine particle behavior, particle-reactive radionuclides such as $^{7}$Be, $^{210}$Pb, $^{234}$Th and $^{137}$Cs have been broadly used to study the dynamics and sources of suspended sediments and to determine the fluxes and rates of internal processes in sedimentary compartments, including rivers, estuaries and oceans (Olsen et al., 1982; Huh et al., 1990; Baskaran et al., 1992; Baskaran and Santschi, 1993; Baskaran and Naidu, 1995; Baskaran et al., 1996a; Chen and Huh, 1999; Smoak et al., 1999, 2000; Su and Huh, 2002; Roos and Valeur, 2006; Liu et al., 2007; Xu et al., 2010; Du et al., 2011; Huang et al., 2010, 2011).

$^{7}$Be ($T_{1/2}$=53.3 day) produced by cosmic ray spallation reactions in the atmosphere is generally delivered to the Earth's surface through wet and dry atmospheric deposition; from there, it is introduced into aquatic systems, where it is quickly adsorbed onto particle surfaces and subsequently removed from the water column in estuarine and coastal environments (Olsen et al., 1986; Baskaran and Santschi, 1993). $^{210}$Pb ($T_{1/2}$=22.3 years) is one of the decay products in the U-series, and it has two components in estuarine and coastal environments; supported $^{210}$Pb and unsupported or excess $^{210}$Pb ($^{210}Pb_{xs}$). An additional source of $^{210}$Pb is from the decay of radon escaped from the soil surface to the

* Corresponding author. Tel.: +86 21 62232761; fax: +86 21 62546441.
*E-mail address:* jzdu@sklec.ecnu.edu.cn (J. Du).

0278-4343/$ - see front matter © 2012 Elsevier Ltd. All rights reserved.
http://dx.doi.org/10.1016/j.csr.2012.04.019

atmosphere, which is then adsorbed onto aerosol particles and deposited over the Earth's surface (Appleby and Oldfield, 1992; Preiss et al., 1996; Du et al., 2008). In the ocean, $^{210}Pb$ is removed by suspended particulate matter and eventually reaches the sediment–water interface. As with $^{210}Pb$ in a marine environment, $^{234}Th$ ($T_{1/2}$=24.3 days) also has two components. The sorbed component of $^{234}Th$ is termed excess $^{234}Th$ ($^{234}Th_{xs}$), while the lattice-bound $^{234}Th$ that is in secular equilibrium with $^{238}U$ is called supported $^{234}Th$. $^{238}U$ activity increases with salinity, and thus, the production rate of $^{234}Th$ also increases with salinity. $^{137}Cs$ ($T_{1/2}$=30.07 years) is produced by thermonuclear bomb testing and the Chernobyl accident. $^{137}Cs$ in surface soils is transferred by eroded fine-grained particles from rivers to oceans (Lima et al., 2005). Taking into account their half-lives, $^{7}Be$ and $^{234}Th_{xs}$ can be used as particle tracers on time scales of days to months. These nuclides are most commonly used for measurements of sediment transport, resuspension, deposition and sediment mixing in aquatic environments (e.g., reservoirs and estuaries) (McKee et al., 1983; Feng et al., 1999a, 1999b; Mckee and Baskaran, 1999; Sommerfield et al., 1999; Wilson et al., 2007). On a time scale from years to decades, sedimentary processes can be determined using $^{137}Cs$ and/or $^{210}Pb$.

Hainan Island, the second largest island of China, is in the south of China and is separated from the mainland by the Qiongzhou Strait (Li et al., 2002; Su and Pohlmann, 2009). The climate on Hainan Island is characterized by tropical monsoons and tropical oceans: offshore winds prevail during the winter monsoon season, while landward winds prevail during the summer monsoon season. Tropical storms and typhoons frequently hit the island in August and September, bringing large amounts of rainfall (Mao et al., 2006). Two estuaries (Wanquan River estuary and Bamen Bay as Fig. 1) and several lagoons enclosed by coral reefs are located on the east coast of Hainan Island. Wanquan River is the third largest river of Hainan, with a discharge of $6.1\times10^{9}$ $m^{3}year^{-1}$. The total annual discharge of the other thirteen large rivers is approximately $1.13\times10^{10}$ $m^{3}$ (Zeng and Zeng, 1989). Upwelling near Hainan Island is concentrated at the east of the island, between 18°30′–20°30′ N and 110°–111°30′ E, which corresponds to the southwesterly and southerly winds circulation in the South China Sea (Deng et al., 1995; Su and Pohlmann, 2009). Thus far, most researches about sedimentation using radionuclides in the South China Sea have been concerned with the south and east of the South China Sea

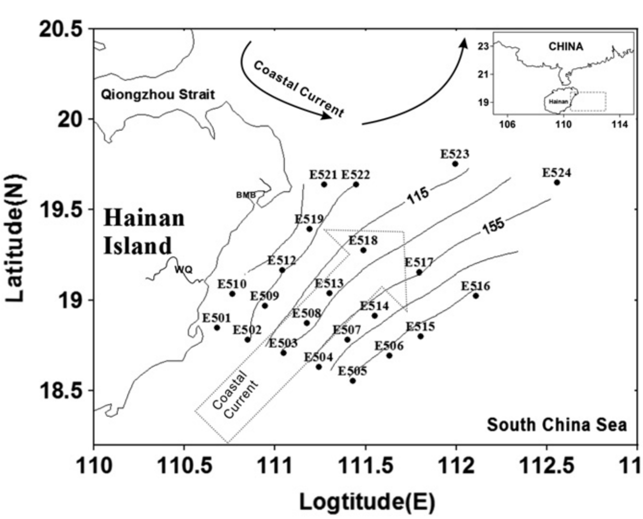


**Fig. 1.** Sampling Locations, the isobaths (m) and current patterns off eastern Hainan, China (WQ: Wanquan River; BMB: Bamen Bay) (Modified from Feng et al., 1999d).

(Liu et al., 2001a, 2001b; Xu et al., 2010). There are few studies about the west of the South China Sea and the east coast of Hainan Island, with its complex current influence, especially on sediment sources and transport processes.

In our previous work, we studied the settling dynamics of suspended particles using $^{7}Be$ and $^{210}Pb$ and the removal rates of heavy metals in the estuaries on the east coast of Hainan (Huang et al., 2011). Here, we extend our previous study from the estuary to offshore of eastern Hainan Island. We determined the activities of $^{7}Be$, $^{210}Pb$, $^{234}Th$ and $^{137}Cs$ in the surface sediments collected at the east coast of Hainan Island, China. The main aims were to study the sediment record of source and transport, which can affect the benthic ecosystem in the environment. The results can provide reference information for similar types along the tropical coasts or for similar hydrodynamic environment. Moreover, knowledge of the sources and transport of sediments can help us more deeply understand the environmental pollution problems (e.g. PCBs, PAHs and heavy metals) in estuary and coastal systems worldwide, and can help us assess pollution risk and plan management strategies (Feng et al., 1999c; Giuliani et al., 2011; Gomez-Gesteira et al., 2011; Huang et al., 2011; Maioli et al., 2011). The remove time in the study region was also obtained, which is information that could be helpful for understanding transport process of pollution.

## 2. Materials and methods

### 2.1. Sample collection

Hainan, a continental-type island, is located in the northwest of the South China Sea. The water depth of the east coast of Hainan decreases greatly, and the isobaths and the coast line are parallel (Fig. 1). The coastal current travels along the Guangdong coastline from east to west in the winter and becomes an anticlockwise loop current; on the eastern offshore, the coastal current travels from south to north in the summer (Feng et al., 1999d). The water depth along the coast decreases sharply with the gradient decreasing from northwest to southeast, the gradient is approximately 0°14′–0°15′ below a depth of 120 m (Deng et al., 1995).

The surface sediments were collected using a grab sampler during two cruises in August, 2008. At each station (Fig. 1), the bottom sediments were sectioned from only the top 0–1 cm of the muddy top layer of the sampled surface sediments.

### 2.2. Analytical methods

The bottom sediments were dried, ground and sealed in 35 mm × 35 mm plastic boxes. The samples were analyzed as quickly as possible after sampling and were analyzed again after nine months. The radioactivities of $^{210}Pb$, $^{226}Ra$, $^{7}Be$, $^{137}Cs$, $^{238}U$ and $^{234}Th$ were measured using an HPGe γ-ray detector (Canberra Be3830) with a 35% counting efficiency and an energy resolution of 1.8 keV (at 1 332 keV) in the multi-layer shielding mode (ultra low background system, 777 lead shields for 12–48 h) (Du et al., 2010; Huang et al., 2010). The activities of $^{7}Be$ and $^{137}Cs$ were determined from the γ-ray peak at 477.6 keV (10.5%) and 661.6 keV (85%), respectively. In this study, the overall activities of $^{210}Pb$ (i.e., supported and excess) were measured from its γ-radiation at 46.5 keV (4.25%). The activity of $^{226}Ra$ was determined at 295.2 keV (19.3%) and 351.9 keV (37.6%) for $^{214}Pb$ and at 609.3 keV (46.1%) and 1120.3 keV (15%) for $^{214}Bi$. $^{234}Th$ and $^{238}U$ were determined from the peak at 63.29 keV (3.72%). The detector systems were calibrated for efficiency using efficiency curves obtained from LabSOCS (Bronson, 2003). Excess $^{234}Th$ ($^{234}Th_{xs}$)

and $^{210}$Pb ($^{210}$Pb$_{xs}$) were obtained by subtracting the estimated parent supported activities from the total activities in the sediments. The reported data for the short-lived nuclides were corrected for the radioactive decay that occurred between sample collection and analysis.

### 2.3. Grain-size, water content and loss on ignition

Grain size ($D$, μm) analyses were carried out on a Colter LS 100Q grain size analyzer, which subdivides each sample into 85 size fractions between 0.3 μm and 1000 μm. The grain size can be expressed using the logarithmic format $\Phi = -\log_2 D$ (Krumbein, 1934). The three sediment components were distinguished by the scope of the size: (1) sand: $-1 < \Phi < 4$; (2) silt: $4 < \Phi < 8$ and (3) clay: $9 < \Phi < 11$ (Liu et al., 2010).

The water content of the samples was determined through drying in an oven at 105 °C to constant weight. The loss on ignition was used as an approximation of the organic matter content in the sediment (TOC). The dry samples were weighed and heated to 550 °C in a muffle furnace for two hours. The samples were weighed again after cooling to room temperature, and the difference was the amount of organic carbon ignited (Dean, 1974; Liu et al., 2007).

## 3. Results and discussions

### 3.1. Sediment characteristics

The geochemical properties of the surface sediments are given in Table 1. The mean grain size of the sediments was 3.30–7.88 ($\Phi$), and the sediments were clay and silt for most of the locations. There was almost no change of mean grain-size from coast to offshore. However, the dominant mineral components of sediments from the northern locations (E519, E521, E522 and E523) were sand (66.4–70.4%), and the grain sizes were much larger than at the other locations. The distribution of grain size showed that the mean grain size of the surface sediments decreased from north to south. Meanwhile, it was found that there were shells in the surface sediments of these locations. As expected, the percentages of water content and TOC showed small values because of the greater sand component in the northern regions. The location of E521 had the largest grain size and the lowest water content and TOC. Because there was a loop current (i.e., part of the Guangdong Coastal Current) at the north coast of Hainan year round (Feng et al., 1999d), the suspended particles with small grain size may have been transported offshore, or there were different sediment sources for the surface sediment of the northern locations (E519, E521, E522 and E523). It can be seen in Table 1 that the percentages of clay and silt in all sediment were 8.6–44.2% and 18.4–77.5%, respectively, whereas the sand content at most stations was almost zero, except at the northern locations (E519, E521, E522 and E523). More detailed analyses of the plots of frequency distribution (%) vs. grain size (Φ) are shown in Fig. 2. Two groups of surface sediments were identified: the samples of the northern area ((E519, E521, E522 and E523) with a grain size of 0–4 ($\Phi$), and the other group, with a grain size of 4–12 ($\Phi$).

### 3.2. The specific activity of radionuclides in the sediments

The activities of $^{7}$Be, $^{210}$Pb$_{xs}$, $^{137}$Cs, $^{234}$Th$_{xs}$, $^{238}$U and $^{226}$Ra in the surface sediments are listed in Table 2, and the distribution is shown in Fig. 3. The activities of $^{7}$Be, $^{210}$Pb$_{xs}$, $^{137}$Cs, $^{234}$Th$_{xs}$, $^{238}$U and $^{226}$Ra were 0.14–12.7, 37.4–199, 0.02–1.06, 2.24–176, 6.0–33.2, and 12.6–25.5 Bq kg$^{-1}$, averaging $3.78 \pm 4.77$, $110 \pm 8.1$, $0.52 \pm 0.22$, $66.7 \pm 8.9$, $21.7 \pm 6.4$ and $19.0 \pm 1.0$ Bq kg$^{-1}$, respectively.

The activities of $^{238}$U and $^{226}$Ra were comparable with the values reported in other coastal systems, and $^{137}$Cs was slightly lower than the values reported in other coastal systems (Allison et al., 2000; Liu et al., 2001a; Hong et al., 2006; Du et al., 2010). The activity of $^{137}$Cs was higher in the middle high latitudes due to rainfall and atmospheric circulation. Also some of the $^{137}$Cs has decayed because its half-life is only 30.07 years. The activities of the $^{210}$Pb$_{xs}$ off eastern Hainan were much higher than the values reported in other coastal systems due to the low sedimentary rate (Allison et al., 2000; Liu et al., 2001a; Du et al., 2010; Dai et al., 2011).

The $^{7}$Be activities were obviously lower than the values reported in other coastal systems (Allison et al., 2000; Palinkas et al., 2005), indicating that the $^{7}$Be needs time to be transported

**Table 1**
Geochemical properties of surface sediments in the east coast of Hainan Island.

| Station | Latitude | Longitude | Depth | Lithology and grain-size parameter | | | | TOC | Water content |
|---|---|---|---|---|---|---|---|---|---|
| | | | m | Clay (%) | Silt (%) | Sand (%) | Mean grain-size ($\Phi$) | % | % |
| **E501** | 18.85 | 110.68 | 90 | 44.2 | 55.8 | 0 | 7.88 | 3.76 | 40.6 |
| **E502** | 18.78 | 110.85 | 92 | 38.1 | 61.9 | 0 | 7.52 | 4.36 | 42.8 |
| **E503** | 18.71 | 111.05 | 139 | 33.4 | 66.6 | 0 | 7.32 | 5.78 | 56.0 |
| **E504** | 18.63 | 111.24 | 163 | 21.3 | 77.5 | 1.2 | 6.51 | 4.79 | 58.9 |
| **E505** | 18.56 | 111.43 | 200 | 28.5 | 71.5 | 0 | 7.04 | 3.59 | 46.6 |
| **E506** | 18.69 | 111.63 | 201 | 29.6 | 70.4 | 0 | 7.12 | 3.63 | 52.3 |
| **E507** | 18.78 | 111.40 | 169 | 17.9 | 72.2 | 9.9 | 6.10 | 3.77 | 52.1 |
| **E508** | 18.87 | 111.18 | 127 | 31.9 | 68.1 | 0 | 7.28 | 4.95 | 67.6 |
| **E509** | 18.97 | 110.94 | 101 | 41.6 | 58.4 | 0 | 7.77 | 4.83 | 56.8 |
| **E510** | 19.04 | 110.76 | 79 | 41.6 | 58.4 | 0 | 7.70 | 2.52 | 40.8 |
| **E512** | 19.17 | 111.04 | 94 | 38.5 | 61.5 | 0 | 7.55 | 2.52 | 33.2 |
| **E513** | 19.04 | 111.30 | 131 | 31.7 | 68.3 | 0 | 7.24 | 4.20 | 55.4 |
| **E514** | 18.92 | 111.55 | 165 | 22.0 | 77.1 | 1.0 | 6.52 | 3.40 | 78.4 |
| **E515** | 18.80 | 111.80 | 205 | 35.8 | 64.2 | 0 | 7.35 | 3.49 | 52.5 |
| **E516** | 19.03 | 112.11 | 200 | 35.9 | 64.1 | 0 | 7.37 | 3.51 | 47.1 |
| **E517** | 19.16 | 111.80 | 153 | 25.5 | 74.5 | 0 | 6.81 | 3.15 | 55.6 |
| **E518** | 19.28 | 111.49 | 126 | 28.3 | 71.7 | 0 | 6.97 | 3.61 | 40.4 |
| **E519** | 19.39 | 111.19 | 90 | 11.3 | 19.1 | 69.6 | 3.60 | 2.23 | 28.9 |
| **E521** | 19.64 | 111.27 | 88 | 11.2 | 18.4 | 70.4 | 3.30 | 2.05 | 29.2 |
| **E522** | 19.64 | 111.45 | 95 | 11.8 | 21.8 | 66.4 | 3.45 | 2.30 | 31.0 |
| **E523** | 19.75 | 111.99 | 107 | 8.6 | 23.9 | 67.5 | 3.79 | 2.58 | 46.2 |
| **E524** | 19.65 | 112.56 | 150 | 29.3 | 70.7 | 0 | 7.02 | 3.22 | 48.4 |

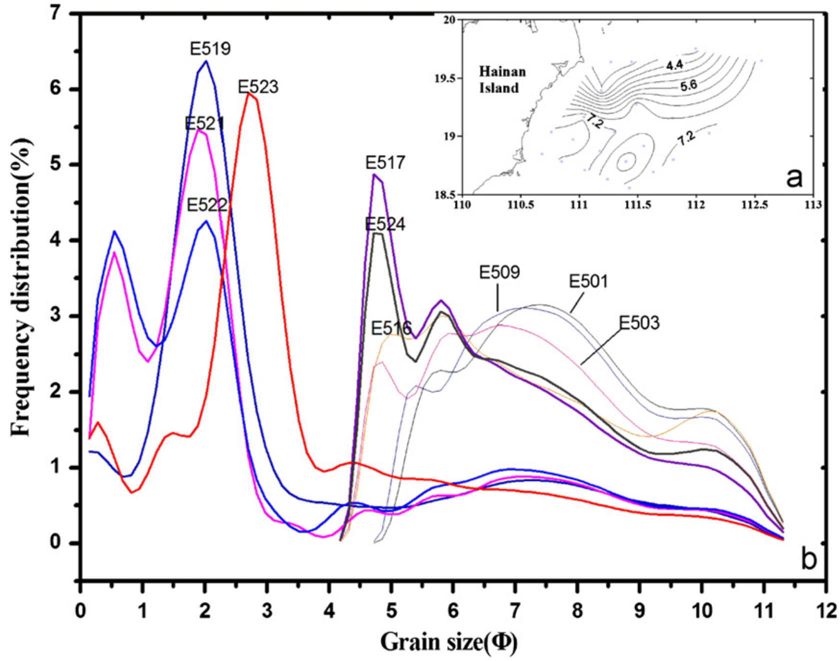


**Fig. 2.** The grain size properties of sediments off eastern Hainan, China: (a) distribution of mean grain size (*Φ*) and (b) frequency percentage of mean grain size in typical surface sediments.

**Table 2**
Radioactivities (Bq kg$^{-1}$) of nuclides in surface sediments off eastern Hainan Island.

| Station | $^{7}$Be | $^{137}$Cs | $^{238}$U | $^{234}$Th$_{xs}$ | $^{226}$Ra | $^{210}$Pb$_{xs}$ |
|---|---|---|---|---|---|---|
| **E501** | – | 0.52 ± 0.21 | 25.1 ± 6.9 | – | 19.7 ± 1.0 | 68.4 ± 5.7 |
| **E502** | 4.26 ± 4.07 | 0.73 ± 0.17 | 16.6 ± 4.7 | 93.1 ± 7.4 | 23.8 ± 1.1 | 81.6 ± 10.7 |
| **E503** | – | 0.44 ± 0.24 | 29.3 ± 8.7 | 137.7 ± 12.6 | 23.8 ± 1.1 | 199.0 ± 12.6 |
| **E504** | 3.01 ± 5.11 | 0.47 ± 0.19 | 12.3 ± 5.6 | 176.0 ± 8.8 | 20.3 ± 1.0 | 170.0 ± 10.8 |
| **E505** | 6.08 ± 3.88 | 0.63 ± 0.16 | 24.2 ± 6.0 | – | 14.5 ± 0.8 | 52.7 ± 4.9 |
| **E506** | – | 1.06 ± 0.24 | 7.8 ± 3.6 | 132.9 ± 6.4 | 14.4 ± 0.8 | 48.9 ± 4.9 |
| **E507** | 3.99 ± 4.46 | – | 22.5 ± 7.0 | 17.7 ± 9.3 | 18.7 ± 1.0 | 145.2 ± 9.5 |
| **E508** | 12.74 ± 5.34 | 0.78 ± 0.27 | 31.6 ± 7.8 | 8.88 ± 10.8 | 24.0 ± 1.1 | 172.1 ± 11.2 |
| **E509** | 0.31 ± 5.92 | 0.80 ± 0.26 | 33.2 ± 8.5 | – | 25.5 ± 1.2 | 144.9 ± 10.0 |
| **E510** | 1.54 ± 5.26 | 0.50 ± 0.19 | 27.4 ± 6.9 | 44.3 ± 10.2 | 22.0 ± 1.1 | 103.2 ± 7.7 |
| **E512** | 0.97 ± 4.46 | 0.33 ± 0.31 | 22.7 ± 6.0 | 15.1 ± 8.6 | 19.1 ± 1.0 | 74.8 ± 6.3 |
| **E513** | 0.44 ± 4.77 | 0.48 ± 0.17 | 26.6 ± 8.3 | – | 20.0 ± 1.0 | 115.4 ± 7.9 |
| **E514** | 10.1 ± 5.23 | 0.71 ± 0.26 | 14.7 ± 5.1 | 104.4 ± 8.0 | 18.6 ± 1.1 | 186.4 ± 11.7 |
| **E515** | – | 0.76 ± 0.19 | 6.0 ± 3.3 | 99.2 ± 5.5 | 14.2 ± 0.8 | 74.0 ± 5.9 |
| **E516** | – | 0.92 ± 0.20 | 11.0 ± 5.9 | 2.24 ± 7.1 | 15.8 ± 0.9 | 48.6 ± 5.0 |
| **E517** | – | 0.30 ± 0.16 | 22.4 ± 6.4 | 18.4 ± 8.7 | 20.3 ± 1.0 | 166.1 ± 10.6 |
| **E518** | – | 0.02 ± 0.27 | 26.8 ± 6.6 | – | 19.9 ± 0.9 | 111.8 ± 7.9 |
| **E519** | – | 0.31 ± 0.18 | 26.5 ± 7.8 | 45.4 ± 10.7 | 22.0 ± 1.0 | 54.0 ± 5.5 |
| **E521** | – | 0.08 ± 0.27 | 20.1 ± 5.3 | – | 12.6 ± 0.8 | 37.4 ± 3.8 |
| **E522** | 0.14 ± 4.51 | – | 21.9 ± 5.6 | – | 18.0 ± 0.9 | 82.6 ± 6.8 |
| **E523** | 1.78 ± 4.20 | – | 22.0 ± 6.4 | – | 17.9 ± 1.0 | 106.7 ± 7.8 |
| **E524** | – | 0.12 ± 0.29 | 26.7 ± 8.0 | 38.2 ± 10.8 | 21.5 ± 1.0 | 194.4 ± 12.0 |

–: Below detection limit.

from the surface water to the bottom of the sea-bed, and most of the $^{7}$Be on the water column had already decayed before it was removed into the seabed.

All the activities of the radionuclides increased from west to east in the north section. The activities of E521 were the smallest of all the locations. As described in section 3.1, E521 has the largest grain size and the lowest water contents and TOC. In the middle of the south section, there was a zone with higher activity, especially at E503 and E504, where the activities of $^{234}$Th$_{xs}$ and $^{210}$Pb$_{xs}$ were higher. It may indicate stronger upwelling around E503 and E504. In the previous work, the particle fluxes were found to be high around the upwelling regions (Shannon et al., 1970; Buesseler et al., 1995; Robert, 1998; Hong et al., 1999). $^{234}$Th and $^{210}$Pb can be scavenged and removed from the water column to the seabed with particles, and the activities of $^{234}$Th$_{xs}$ and $^{210}$Pb$_{xs}$ were higher.

### 3.3. *Relationships among nuclide activity and other geochemical properties in the surface sediments*

To further examine the extent of radioactivity and geochemical properties, the results of the linear relationship analysis among geochemical properties and activities of nuclides in surface sediments are shown in Table 3. The correlation coefficient of $^{7}$Be and $^{137}$Cs was the highest. $^{210}$Pb$_{xs}$ also had a high correlation with $^{7}$Be and $^{137}$Cs. All three nuclides originated from wet and dry

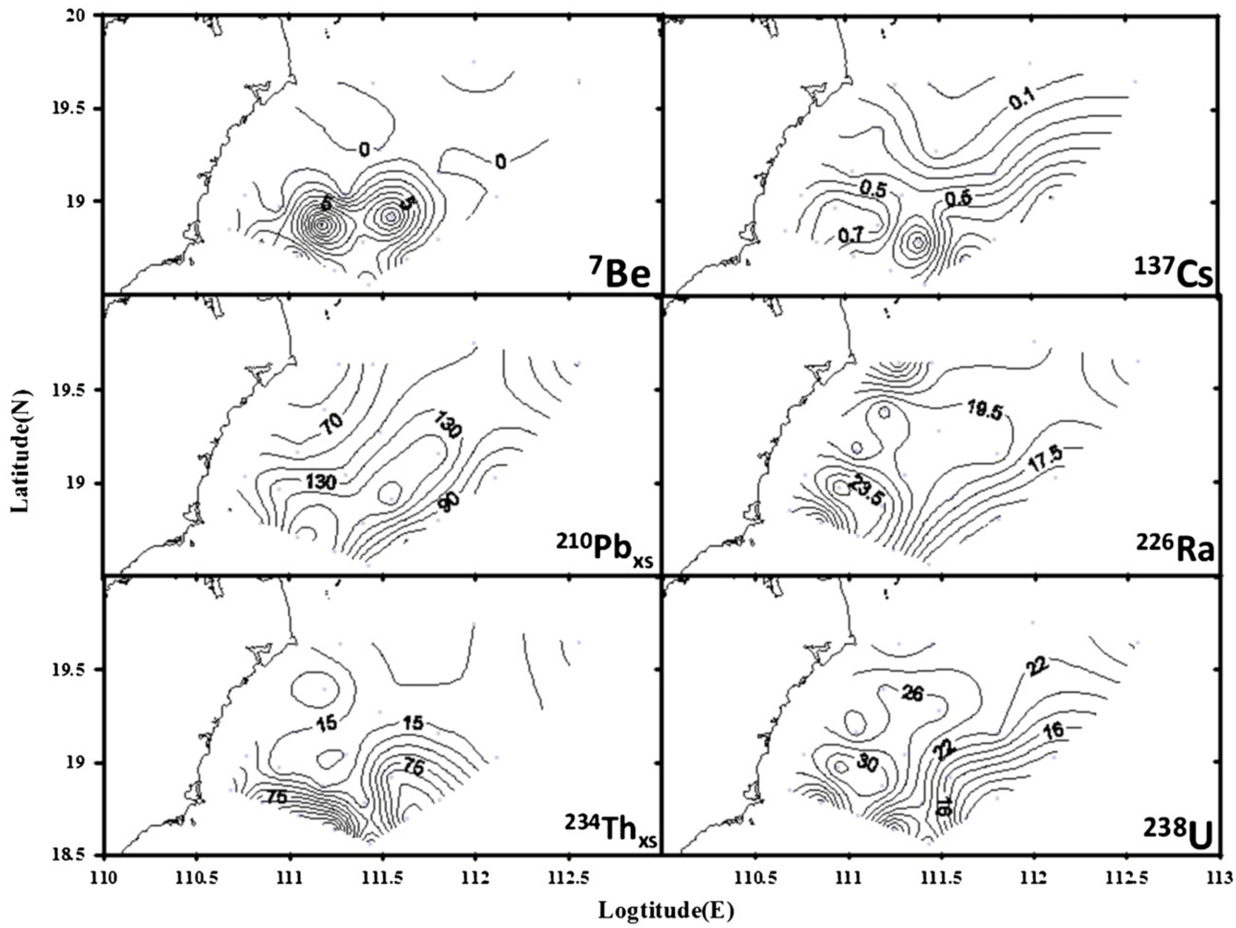


**Fig. 3.** The distribution of radionuclide activities in surface sediments (Bq kg$^{-1}$).

**Table 3**
Linear correlation coefficients between mean grain size (μm), TOC (%) and radioactivities of nuclides (Bq kg$^{-1}$) in sediments ($n$=22).

| | Grain size | TOC | $^{7}$Be | $^{137}$Cs | $^{226}$Ra | $^{234}$Th$_{xs}$ | $^{210}$Pb$_{xs}$ | $^{238}$U |
|---|---|---|---|---|---|---|---|---|
| Grain size | 1.000 | | | | | | | |
| TOC | 0.379 | 1.000 | | | | | | |
| $^{7}$Be | 0.272 | 0.567 | 1.000 | | | | | |
| $^{137}$Cs | 0.203 | 0.557 | 0.947 | 1.000 | | | | |
| $^{226}$Ra | −0.010 | 0.026 | 0.191 | 0.131 | 1.000 | | | |
| $^{234}$Th$_{xs}$ | 0.878 | 0.286 | −0.134 | −0.112 | −0.044 | 1.000 | | |
| $^{210}$Pb$_{xs}$ | 0.777 | 0.391 | 0.570 | 0.488 | 0.558 | 0.558 | 1.000 | |
| $^{238}$U | −0.688 | −0.181 | 0.186 | 0.173 | 0.679 | −0.750 | −0.083 | 1.000 |

atmospheric deposition or the terrigenous clasts delivered by floods. The correlation coefficients between U-series nuclides were also higher, and $^{210}$Pb$_{xs}$ also has a high correlation with $^{234}$Th$_{xs}$.

It can be seen in Table 3 that there are two groups of particle-reactive nuclides: $^{7}$Be and $^{137}$Cs have a stronger relationship with TOC than $^{234}$Th$_{xs}$ and $^{210}$Pb$_{xs}$, but $^{234}$Th$_{xs}$ and $^{210}$Pb$_{xs}$ have a much higher linear coefficient with the mean grain particle size than $^{7}$Be and $^{137}$Cs. $^{210}$Pb$_{xs}$ and $^{234}$Th$_{xs}$ have stronger affinities with non-biological particles than biogenic particles (Baskaran et al., 1996a; Baskaran and Santschi, 2002). Also, the association of $^{137}$Cs with fine particle and sediment organic carbon content has been well known in the coastal sediments (Baskaran et al., 1996b; Hong et al., 2006). This phenomenon suggests that their removal behaviors may be different, i.e., $^{7}$Be and $^{137}$Cs have a greater tendency to be removed from the water column by biogenic particles, while $^{210}$Pb$_{xs}$ and $^{234}$Th$_{xs}$ have a greater tendency to be removed by inorganic particles, and these differences can be recorded in the sediments.

To further understand the relationship of the locations and the hydrodynamics in the study area, a hierarchical clustering analysis of the data was performed with the distance metrics based on the Euclidean distance single linkage method (Gotelli and Ellison, 2004; Zhang et al., 2009). The results shown in Fig. 4 indicated that E521 had a more distant association with other locations. At E521, the grain size was the largest, while TOC, $^{7}$Be, $^{210}$Pb$_{xs}$, $^{137}$Cs, $^{234}$Th$_{xs}$ and $^{226}$Ra were the lowest. E519, E522 and E523 were close to E521 and differed more from the other locations, which indicates that the geochemical properties and radioactivities of the northern locations were different and were affected more by the loop current (Guangdong Coastal Current). The Hainan Coastal Current travels from south to north in the summer, as shown in Fig. 1 (Chu et al., 1999; Feng et al., 1999d). The activities of radionuclides and other geochemical properties in the sediments of

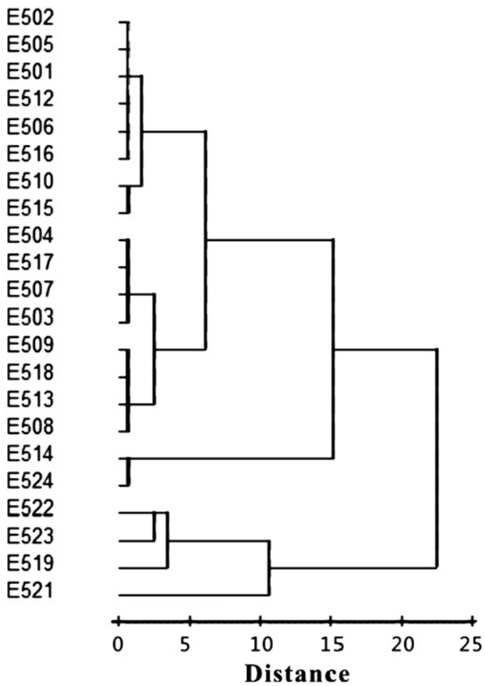


**Fig. 4.** Hierarchical clustering analysis shows the relevant associations among the locations.

the north and south locations can be influenced by different hydrodynamic situations and produce different recorded characteristics.

### 3.4. The radioactivity ratio in the sediments and the source and transport of the sediments

The radionuclides and the ratios in suspended sediment and sediment has been used to investigate their transport and source (Feng et al., 1999b; Huh and Su, 1999; Wilson et al., 2007).

The distribution of radionuclide ratio is shown in Fig. 5. The ratio of $^{7}Be/^{210}Pb_{xs}$ decreased from west to east (seaward), indicating that the land source of these particles may affect this region more heavily near-shore (Fan et al., 1987; Xu et al., 2008). However, both $^{137}Cs/^{210}Pb_{xs}$ and $^{234}Th_{xs}/^{210}Pb_{xs}$ increased seaward, suggesting that $^{137}Cs$ (with $^{234}Th_{xs}$ definitely coming from seaward) may be coming from the west Pacific Ocean or from local production, then being deposited with the settling of suspended particles in the regions. A similar phenomenon has been also observed in other estuaries and coasts (Hong et al., 2006; Du et al., 2010). $^{234}Th$ and $^{137}Cs$ would be more easily resuspended as they follow the fine sediments, and some of the sediments may have been transported by the Hainan Coastal Current (part of the Viet Nam Coastal Current) and taken to the western locations from offshore with the upwelling.

The $^{7}Be$ activities were obviously lower than the values reported in other coastal systems, it may indicated that either fewer particles came from the river discharge or the transport of the river-discharged particles to sea-bed required more time. The age of the sediments and the removal time of the suspended particles from the water column to the seabed can be calculated using the nuclide activity ratio. $^{7}Be/^{210}Pb$ ($^{210}Pb$ was excess $^{210}Pb$.) can be used to calculate the age ($t$) of the sediment as the following equation (Matisoff et al., 2005; Saari et al., 2010):

$$t = \frac{1}{\lambda_{^7Be} - \lambda_{^{210}Pb}} \ln(^{7}Be/^{210}Pb) + \frac{1}{\lambda_{^7Be} - \lambda_{^{210}Pb}} \ln(^{7}Be/^{210}Pb)_0 \qquad (1)$$

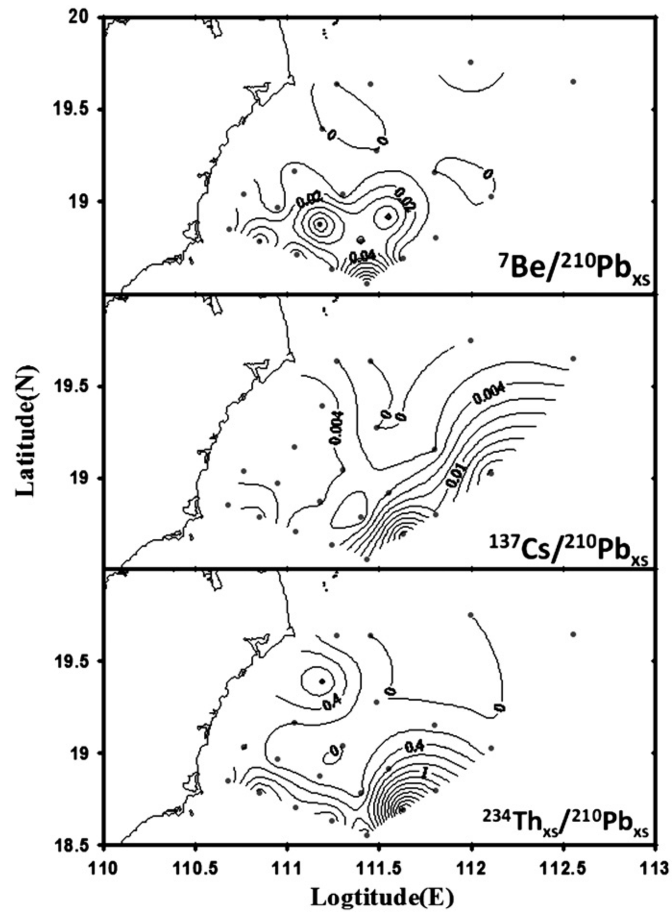


**Fig. 5.** Activity ratios of the radionuclides of the surface sediments off eastern Hainan Island.

where $\lambda_{^7Be}$ and $\lambda_{^{210}Pb}$ are the decay constants of $^{7}Be$ and $^{210}Pb$, respectively, ($^{7}Be/^{210}Pb$) is the $^{7}Be/^{210}Pb$ ratio of the sediment, and $(^{7}Be/^{210}Pb)_0$ is the $^{7}Be/^{210}Pb$ ratio of the atmospheric deposition or the suspended sediment in the surface water. The $^{7}Be/^{210}Pb$ of atmospheric deposition was approximately 3.28 in the study regions (Huang et al., 2011). The $^{7}Be/^{210}Pb$ of the surface sediments at the east coast ranged from 0.002 to 0.074, averaging 0.034. The calculated surface sediment age was approximately 1 year. By contrast, the $^{7}Be/^{210}Pb$ of the suspended sediments in the Bamen Bay and the Wanquan River estuary in the Hainan Island ranged from 0.08 to 3.60, averaging 1.15 (Huang et al., 2011). We assumed that the $^{7}Be/^{210}Pb$ of the suspended sediments in the surface water was same as the $^{7}Be/^{210}Pb$ of the suspended sediments in the estuaries. Also, the surface sediment age calculated using the $^{7}Be/^{210}Pb$ of the suspended sediments was approximately 9 months, which indicates that the suspended particles in the water column may take 9–12 months to be removed from the water column and transported into the sea-bed. However, the activities of $^{7}Be$ in many locations were below the lower limit of detection, which indicates that the age of the sediments was more than 9 months in some regions.

The $^{226}Ra$ in the deep sea sediments was higher because $^{230}Th$ can be removed from the water (Kroll, 1953; Pettersson, 1955; Ivanovich and Harmon, 1992). The disequilibria of $^{226}Ra$ and $^{238}U$ can also give some evidence for the source of the surface sediments on a long time scale. The activities of $^{226}Ra$ vs. $^{238}U$ in the surface sediments of the east coast of Hainan, the Guangdong coast, river and continental slope were detected (Fig. 6). The $^{238}U$ activities of all the surface sediments ranged from 6.0

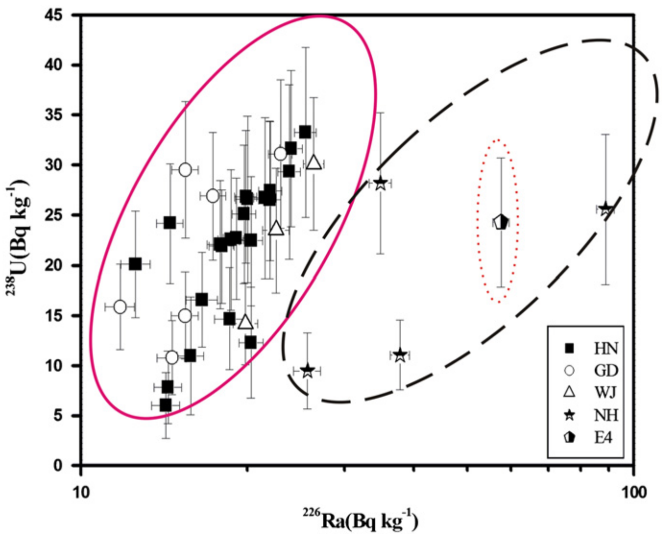


**Fig. 6.** $^{226}$Ra vs. $^{238}$U in the surface sediments (HN: sediments off the eastern coast of Hainan; GD: sediments along the Guangdong coast at a depth of 40–175 m; WJ: sediments in the Wenjiao River of Bamen Bay; NH: surface sediments on the continental slope near the Guangdong coast at a depth 670–2300 m; E4 (18°N; 110°E): surface sediments to the south of Hainan. NH and E4 are on the pathway of the warm current of the South China Sea).

to 33.2, and the $^{226}$Ra activities ranged from 11.8 to 88.8 Bq kg$^{-1}$. Obviously, the $^{226}$Ra/$^{238}$U of sediments in the continental slope locations (NH and E4) which is located on the continental slope with the warm current of South China Sea and the water depths is more than 670 m, were higher than those in the other locations off eastern Hainan Island. Moreover, the $^{226}$Ra/$^{238}$U in sediments off eastern Hainan Island (except NH and E4) were comparable with those in the sediments of Guangdong coast and river where the sediments are generally thought with terrigenous characteristics. Therefore, we speculate that the main source of the sediments off eastern Hainan Island was terrigenous deposition.

## 4. Conclusions

Bottom sediments collected in August of 2008 from 22 stations off eastern Hainan Island were analyzed for several decay-series nuclides, $^{7}$Be and $^{137}$Cs. From the present investigation, the following conclusions can be drawn:

1. The source and the transport processes of the surface sediments can be well characterized by multiple radionuclides as tracers. The removal mechanisms of four particle reactive nuclides are different: $^{7}$Be and $^{137}$Cs can be more easily removed in the water column by biological particles; $^{210}Pb_{xs}$ and $^{234}Th_{xs}$ can reflect the removal of non-biological particles with a small grain size. The activities of $^{210}Pb_{xs}$ and $^{234}Th_{xs}$ were found to be higher in the southern upwelling regions, which had higher particle fluxes.
2. Both the coastal current and the upwelling strongly affect the sediment source, transport and deposition processes: the sediment source of the study regions was mainly terrigenous deposits and the sediment can be transported by the Hainan Coastal Current (from south to north).
3. More than nine months is required for the suspended particles in the water column to be removed and transported to the seabed.

## Acknowledgments

This study was carried out within the frame of the bilateral Sino-German research project LANCET funded jointly by the Chinese Ministry of Science and Technology (2007DFB20380) and the German Federal Ministry of Education and Research (FKZ03S0457A; FKZ03F0620A). D.K. Huang was supported by the ECNU Reward for Excellent Doctors in Academics (XRZZ2011020). We are grateful to editors and three anonymous reviewers for their constructive comments, which improved our manuscript.

## References

Allison, M.A., Kineke, G.C., Gordon, E.S., Goni, M.A., 2000. Development and reworking of a seasonal flood deposit on the inner continental shelf off the Atchafalaya River. Continental Shelf Research 20 (16), 2267–2294.
Appleby, P.G., Oldfield, F., 1992. Application of $^{210}$Pb to sedimentation studies. In: Ivanovich, M., Harmon, R.S. (Eds.), Uranium-Series Disequilibrium: Applications to Earth, Marine, and Environmental Sciences. Clarendon, Oxford, pp. 731–778.
Baskaran, M., Naidu, A.S., 1995. $^{210}$Pb-derived chronology and the fluxes of $^{210}$Pb and $^{137}$Cs isotopes into continental shelf sediments, Rast Chukchi Sea, Alaskan Arctic. Geochimica Cosmochimica Acta 59 (21), 4435–4448.
Baskaran, M., Santschi, P.H., 1993. The role of particles and colloids in the transport of radionuclides in coastal environments of Texas. Marine Chemistry 43 (1–4), 95–114.
Baskaran, M., Santschi, P.H., 2002. Particulate and dissolved Pb-210 activities in the shelf and slope regions of the Gulf of Mexico waters. Continental Shelf Research 22 (10), 1493–1510.
Baskaran, M., Santschi, P.H., Benoit, G., Honeyman, B.D., 1992. Scavenging of thorium isotopes by colloids in seawater of the Gulf of Mexico. Geochimica Cosmochimica Acta 56, 3375–3388.
Baskaran, M., Santschi, P.H., Guo, L., Bianchi, T.S., Lambert, C., 1996a. $^{234}$Th:$^{238}$U disequilibria in the Gulf of Mexico: the importance of organic matter and particle concentration. Continental Shelf Research 16 (3), 353–380.
Baskaran, M., Asbill, S., Santschi, P.H., Brooks, J., Champ, M., Adkinson, D., Colmer, M.R., Makeyev, V., 1996b. Pu, $^{137}$Cs, and excess $^{210}$Pb in the Russian Arctic Sediments. Earth and Planetary Science Letters 140, 243–257.
Bronson, F., 2003. Validation of the accuracy of the LabSOCS software for mathematical efficiency calibration of Ge detectors for typical laboratory samples. Journal of Radioanalytical and Nuclear Chemistry 255 (1), 137–141.
Burnett, W.C., Peterson, R., Moore, W.S., de Oliveira, J., 2008. Radon and radium isotopes as tracers of submarine groundwater discharge—results from the Ubatuba, Brazil SGD assessment intercomparison. Estuarine, Coastal and Shelf Science 76 (3), 501–511.
Buesseler, K.O., Andrews, J.A., Hartman, M.C., Belastock, R., Chai, F., 1995. Regional estimates of the export flux of particulate organic carbon derived from thorium-234 during the JGOFS EqPac program. Deep Sea Research Part II: Topical Studies in Oceanography 42 (2–3), 777–791.
Chen, H.Y., Huh, C.A., 1999. Th-232-Ra-228-Th-228 disequilibrium in East China Sea sediments. Journal of Environmental Radioactivity 42 (1), 93–100.
Chu, P.C., Edmons, N.L., Fan, C., 1999. Dynamical mechanisms for the South China Sea seasonal circulation and thermohaline variabilitie. Journal of Physical Oceanography 29 (11), 2971–2989.
Dai, Z.J., Du, J.Z., Chu, A., Zhang, X.L., 2011. Sediment characteristics in the North Branch of the Yangtze Estuary based on radioisotope tracers. Environmental Earth Sciences 62 (8), 1629–1634.
Dean, W.E., 1974. Determination of carbonate and organic matter in calcareous sediments and sedimentary rocks by loss on ignition; comparison with other methods. Journal of Sedimentary Research 44 (1), 242–248.
Deng, S., Zhong, H., Wang, M., Yun, F., 1995. On relation between upwelling off Qionghai and fishery. Journal of Oceanography in Taiwan Strait 14 (1), 51–56.
Du, J., Zhang, J., Zhang, J., Wu, Y., 2008. Deposition patterns of atmospheric $^{7}$Be and $^{210}$Pb in coast of East China Sea, Shanghai, China. Atmospheric Environment 42 (20), 5101–5109.
Du, J., Wu, Y., Huang, D., Zhang, J., 2010. Use of $^{7}$Be, $^{210}$Pb and $^{137}$Cs tracers to the transport of surface sediments of the Changjiang Estuary, China. Journal of Marine Systems 82 (4), 286–294.
Du, J.Z., Zhang, J., Baskaran, M., 2011. Applications of short-lived radionuclides ($^{7}$Be, $^{210}$Pb, $^{210}$Po, $^{137}$Cs and $^{234}$Th) to trace the sources, transport pathways, and deposition of particles/sediments in rivers, estuaries and coasts.. In: Baskaran, M. (Ed.), Handbook of Environmental Isotope Geochemistry. Springer, pp. 305–330.
Fan, S., Luo, Y., Guo, Z., Hu, D., 1987. Bottom sediment zonation of the South China Sea. Nanhai Studia Marina Sinica 8, 55–60.
Feng, H., Cochran, J.K., Hirschberg, D.J., 1999a. $^{234}$Th and $^{7}$Be as tracers for the transport and dynamics of suspended particles in a partially mixed estuary. Geochimica Et Cosmochimica Acta 63 (17), 2487–2505.
Feng, H., Cochran, J.K., Hirschberg, D.J., 1999b. Th-234 and Be-7 as tracers for the sources of particles to the turbidity maximum of the Hudson River estuary. Estuarine Coastal and Shelf Science 49 (5), 629–645.

Feng, H., Cochran, J.K., Hirschberg, D.J., 1999c. $^{234}$Th and $^{7}$Be as tracers for transport and sources of particle-associated contaminants in the Hudson River estuary. The Science of The Total Environment 237-238, 401–418.

Feng, S., Li, F., Li, S., 1999d. An Introduction to Marine Science. Higher Education Press, Beijing (in Chinese).

Gotelli, N.J., Ellison, A.M., 2004. A Primer of Ecological Statistics. Sinauer Associates, Sunderland, Massachusetts, USA.

Giuliani, S., Piazza, R., Bellucci, L.G., Cu, N.H., Vecchiato, M., Romano, S., Mugnai, C., Nhon, D.H., Frignani, M., 2011. PCBs in Central Vietnam coastal lagoons: levels and trends in dynamic environments. Marine Pollution Bulletin 62 (5), 1013–1024.

Gomez-Gesteira, M., Beiras, R., Presa, P., Vilas, F., 2011. Coastal processes in northwestern Iberia, Spain. Continental Shelf Research 31 (5), 367–375.

Hong, G.-H., Park, S.K., Baskaran, M., Kim, S.H., Chung, C.S., Lee, S.H., 1999. Lead-210 and polonium-210 in the winter well-mixed waters in the mouth of the Yellow Sea. Continental Shelf Research 19, 1049–1064.

Hong, G.H., Chung, C.S., Lee, S.-H., Kim, S.H., Baskaran, M., Lee, H.M., Kim, Y.I., Yang, D.B., Kim, C.K., 2006. Artificial radionuclides in the Yellow Sea: inputs and redistribution. Radioactivity In The Environment 8, 96–113.

Huang, D., Du, J., Wu, Y., Li, D., Zhang, J., 2010. Sinking of particulate $^{234}Th_{xs}$, $^{7}$Be and $^{210}Pb_{xs}$ in the Changjiang estuary, China. Chinese Journal of Oceanology and Limnology 28 (6), 1152–1159.

Huang, D., Du, J., Zhang, J., 2011. Particle dynamics of $^{7}$Be, $^{210}$Pb and the implications of sedimentation of heavy metals in the Wenjiao/Wenchang and Wanquan River estuaries, Hainan, China. Estuarine, Coastal and Shelf Science 93 (4), 431–437.

Huh, C.A., Small, L.F., Niemnil, S., Finney, B.P., Hickey, B.M., Kachel, N.B., Gorsline, D.S., Williams, P.M., 1990. Sedimentation dynamics in the Santa Monica-San Pedro Basin off Los Angeles: radiochemical, sediment trap and transmissometer studies. Continental Shelf Research 10 (2), 137–164.

Huh, C.A., Su, C.C., 1999. Sedimentation dynamics in the East China Sea elucidated from $^{210}$Pb, $^{137}$Cs and $^{239,240}$Pu. Marine Geology 160 (1-2), 183–196.

Ivanovich, M., Harmon, R.S., 1992. Uranium-series Disequilibrium: Application to Earth, Marine and Environmental Sciences. Clarendon Press, Oxford pp. 407–408.

Kroll, V., 1953. Vertical Distribution of Radium in Deep-Sea Sediments. Nature 171, 742.

Krumbein, W.C., 1934. Size frequency distributions of sediments. Journal of Sedimentary Research 4 (2), 65–77.

Li, X.H., Zhou, H., Chung, S.L., Ding, S., Liu, Y., Lee, C.Y., Ge, W., Zhang, Y., Zhang, R., 2002. Geochemical and Sm–Nd isotopic characteristics of metabasites from central Hainan Island, South China and their tectonic significance. Island Arc 11 (3), 193–205.

Lima, A.L., Hubeny, J.B., Reddy, C.M., King, J.W., Hughen, K.A., Eglinton, T.I., 2005. High-resolution historical records from Pettaquamscutt River basin sediments: 1. $^{210}$Pb and varve chronologies validate record of $^{137}$Cs released by the Chernobyl accident. Geochimica Et Cosmochimica Acta 69 (7), 1803–1812.

Liu, G., Huang, Y., Chen, M., Qiu, Y., 2001a. Distribution features of radionuclides in surface sediments of Nansha Sha Sea. Marine Sciences 25 (8), 1–5.

Liu, G., Huang, Y., Chen, M., Qiu, Y., Cai, Y., Gao, Z., 2001b. Specif ic activity and distribution of natural radionucl ides and $^{137}$Cs in surface sediments of the northeastern South China Sea. Acta Oceanologica Sinica 23 (6), 76–84.

Liu, G., Liu, S., Zhang, J., Huang, Y., Chen, M., 2007. Sedimentary processes of the qingdao nearshore traced using a multi-radionuclide approach. Water, Air, & Soil Pollution: Focus 7 (6), 693–701.

Liu, H., He, Q., Wang, Z., Weltje, G.J., Zhang, J., 2010. Dynamics and spatial variability of near-bottom sediment exchange in the Yangtze Estuary, China. Estuarine, Coastal and Shelf Science 86 (3), 322–330.

Maioli, O.L.G., Rodrigues, K.C., Knoppers, B.A., Azevedo, D.A., 2011. Distribution and sources of aliphatic and polycyclic aromatic hydrocarbons in suspended particulate matter in water from two Brazilian estuarine systems. Continental Shelf Research 31 (10), 1116–1127.

Mao, L., Zhang, Y., Bi, H., 2006. Modern pollen deposits in coastal mangrove swamps from Northern Hainan Island, China. Journal of Coastal Research 22 (6), 1423–1436.

Matisoff, G., Wilson, C.G., Whiting, P.J., 2005. The Be-7/Pb-210(xs) ratio as an indicator of suspended sediment age or fraction new sediment in suspension. Earth Surface Processes and Landforms 30 (9), 1191–1201.

Mckee, B.A., Baskaran, M., 1999. Sedimentary processes of Gulf of Mexico estuaries. In: Bianchi, T.S., Pennock, J.R., Twilley, R.R. (Eds.), Biogeochemistry of Gulf of Mexico Estuaries. Wiley, New York, pp. 63–85.

McKee, B.A., Nittrouer, C.A., DeMaster, D.J., 1983. Concepts of sediment deposition and accumulation applied to the continental shelf near the mouth of the Yangtze River. Geology 11 (11), 631–633.

Moore, W.S., de Oliveira, J., 2008. Determination of residence time and mixing processes of the Ubatuba, Brazil, inner shelf waters using natural Ra isotopes. Estuarine Coastal and Shelf Science 76 (3), 512–521.

Olsen, C.R., Cutshall, N.H., Larsen, I.L., 1982. Pollutant—particle associations and dynamics in coastal marine environments: a review. Marine Chemistry 11 (6), 501–533.

Olsen, C.R., Larsen, I.L., Lowry, P.D., Cutshall, N.H., Nichols, M.M., 1986. Geochemistry and deposition of $^{7}$Be in riverestuarine and coastal waters. Journal of Geophysical Research 91 (C1), 896–908.

Palinkas, C.M., Nittrouer, C.A., Wheatcroft, R.A., Langone, L., 2005. The use of $^{7}$Be to identify event and seasonal sedimentation near the Po River delta, Adriatic Sea. Marine Geology 222–223, 95–112.

Pettersson, H., 1955. Radium and deep-sea chronology. Nature 167, 942.

Preiss, N., Mélières, M.-A., Pourchet, M., 1996. A compilation of data on lead-210 concentration in surface air and fluxes at the air-surface and water-sediment interfaces. Journal of Geophysical Research 101 (D22), 28847–28862.

Robert, C.T., 1998. Particle fluxes in a coastal upwelling zone: sediment trap results from Santa Barbara Basin, California. Deep Sea Research Part II: Topical Studies in Oceanography 45 (8–9), 1863–1884.

Roos, P., Valeur, J.R., 2006. A sediment trap and radioisotope study to determine resuspension of particle reactive substances in the sound between Sweden and Denmark. Continental Shelf Research 26 (4), 474–487.

Saari, H.K., Schmidt, S., Castaing, P., Blanc, G., Sautour, B., Masson, O., Cochran, J.K., 2010. The particulate $^{7}Be/^{210}Pb_{xs}$ and $^{234}Th/^{210}Pb_{xs}$ activity ratios as tracers for tidal-to-seasonal particle dynamics in the Gironde estuary (France): Implications for the budget of particle-associated contaminants. Science of the Total Environment 408 (20), 4784–4794.

Sanford, L.P., 1992. New sedimentation, resuspension, and burial. Limnology and Oceanography 37 (6), 1164–1178.

Santschi, P.H., Guo, L., Walsh, I.D., Quigley, M.S., Baskaran, M., 1999. Boundary exchange and scavenging of radionuclides in continental margin waters of the Middle Atlantic Bight: implications for organic carbon fluxes. Continental Shelf Research 19 (5), 609–636.

Shannon, L.V., Cherry, R.D., Orren, M.J., 1970. Polonium-210 and lead-210 in the marine environment. Geochimica et Cosmochimica Acta 34 (6), 701–711.

Smoak, J.M., Moore, W.S., Thunell, R.C., 2000. Influence of boundary scavenging and sediment focusing on Th-234, Th-228 and Pb-210 fluxes in the Santa Barbara Basin. Estuarine Coastal and Shelf Science 51 (3), 373–384.

Smoak, J.M., Moore, W.S., Thunell, R.C., Shaw, T.J., 1999. Comparison of Th-234, Th-228, and Pb-210 fluxes with fluxes of major sediment components in the Guaymas Basin, Gulf of California. Marine Chemistry 65 (3–4), 177–194.

Sommerfield, C.K., Nittrouer, C.A., Alexander, C.R., 1999. Be-7 as a tracer of flood sedimentation on the northern California continental margin. Continental Shelf Research 19 (3), 335–361.

Su, C.C., Huh, C.A., 2002. $^{210}$Pb, $^{137}$Cs and $^{239,240}$Pu in East China Sea sediments: sources, pathways and budgets of sediments and radionuclides. Marine Geology 183 (1–4), 163–178.

Su, J., Pohlmann, T., 2009. Wind and topography influence on an upwelling system at the eastern Hainan coast. Journal of Geophysical Research 114 (C6), C06017.

Su, N., Du, J., Moore, W.S., Liu, S., Zhang, J., 2011. An examination of groundwater discharge and the associated nutrient fluxes into the estuaries of eastern Hainan Island, China using $^{226}$Ra. Science of the Total Environment 409 (19), 3909–3918.

Wilson, C.G., Matisoff, G., Whitng, P.J., 2007. The use of Be-7 and Pb-210(xs) to differentiate fine suspended sediment sources in South Slough, Oregon. Estuaries and Coasts 30 (2), 348–358.

Xu, D., Long, J., Qian, J., Xi, P., 2008. The modern sedimentation rate and the distribution character of 7 cores in Hainan Island offshore. Journal of Marine Sciences 26 (3), 9–17.

Xu, L.Q., Liu, X.D., Sun, L.G., Yan, H., Liu, Y., Luo, Y.H., Huang, J., Wang, Y.H., 2010. Distribution of radionuclides in the guano sediments of Xisha Islands, South China Sea and its implication. Journal of Environmental Radioactivity 101 (5), 362–368.

Yeager, K.M., Santschi, P.H., Rowe, G.T., 2004. Sediment accumulation and radionuclide inventories (Pu-239, Pu-240, Pb-210 and Th-234) in the northern Gulf of Mexico, as influenced by organic matter and macrofaunal density. Marine Chemistry 91 (1–4), 1–14.

Zeng, Z.X., Zeng, X.Z., 1989. Physicogeography of Hainan Island. Science Press, Beijing (in Chinese).

Zhang, W., Feng, H., Chang, J., Qu, J., Xie, H., Yu, L., 2009. Heavy metal contamination in surface sediments of Yangtze River intertidal zone: an assessment from different indexes. Environmental Pollution 157 (5), 1533–1543.